corroborates the claim made in the Raman work of the existence of the Np(V) dimer.[10] Since the dimer forms at Np(V) concentrations $\gtrsim$0.2 M, solution 4, with 0.5 M Np(V), should also display a peak at 4.2 Å, albeit much smaller than that seen for solution 3.

Equilibrium constants, K/Γ, for the Np(V)-U(VI) complex and Np(V) dimer were determined by us in ref 10. The concentrations of actinyl ions and the cation-cation complex for solutions 1-5 were calculated with these K/Γ values. We note that there is a qualitative correlation between the relative intensities of the peaks at 1.8 and 4.2 Å and these calculated concentrations, as listed in Table I. Because the intensities of the peaks in the $G(r)$ functions are small, their dependene upon the concentration of the complex cannot be established quantitatively.

Another point of interest concerning the radial distribution functions in Figure 2 is that the association of water molecules in the solution—the so-called "water structure", as exemplified by the O-O intermolecular water-water distance at 2.9 Å—is seen in solutions 4 and 5, which contain only $Np_2O_2ClO_4$ or $UO_2(ClO_4)_2$ at relatively low concentrations, 0.5 M. This feature of the $G(r)$ function is not seen in solutions 1-3. It may be that the presence of the cation-cation complex or the high concentrations of ClO_4^- ion disrupt this feature of aqueous solutions.

It is noteworthy that the actinide-actinide distance that we find, 4.2 Å, is comparable to the value of 3.9 Å reported as the U-U distance for solutions and solids containing polymers of hydrolyzed UO_2^{2+} species.[14,16,17] A point of distinction between the two sets of results is that the uranium atoms in the polymers are joined by OH^- bridges, while the cation-cation complexes are formed in strongly acidic media, where hydrolysis is not possible. The large distance, 4.2 Å, does indicate that the metal ions are not directly bonded to each other. This distance, along with the 1.8-Å value for An-O, does not define a unique structure for the actinide cation-cation complex. As discussed in ref 10, at least two models have previously been suggested for the complex, in which the actinide ions are linked either via the axial oxygen of the actinyl(1+) ion or through the oxygen atom of some ligand such as ClO_4^- or H_2O. Both models are consistent with our data. Thus, while the present work has provided supporting evidence for the existence of the cation-cation complexes, further studies are required to define their structure.

Acknowledgment. This work was sponsored by the Divisions of Chemical Sciences and Materials Sciences, Office of Basic Energy Sciences, U.S. Department of Energy, under Contract W-7405-eng-26 with Union Carbide Corp., and by the Centre d'Etudes Nucléaires, Fontenay-aux-Roses, France. We wish to thank J. S. Johnson for suggesting this experimental approach to B.G. and R.L.H. and acknowledge C. F. Baes and J. H. Burns for interesting discussions about this subject. B.G. wishes to thank the Chemistry Division of Oak Ridge National Laboratory for the hospitality received during his stay and the Centre d'Etudes Nucléaires of Fontenay-aux-Roses for support while this project was carried out at ORNL.

Registry No. $NpO_2(ClO_4)$, 83477-23-0; $UO_2(ClO_4)_2$, 13093-00-0.

---

(16) M. Åberg, *Acta Chem. Scand.*, **24**, 2901 (1970).

(17) C. Musikas and A. H. Narten, *Inorg. Nucl. Chem. Lett.*, **14**, 283 (1978).

Contribution from the Molecular Research Institute, Palo Alto, California 94304, and
the Extraterrestrial Research Division, NASA-Ames Research Center, Moffett Field, California 94035

Interaction of Metal Ions and Amino Acids: Possible Mechanisms for the Adsorption of Amino Acids on Homoionic Smectite Clays

ABHA GUPTA, GILDA H. LOEW,* and JAMES LAWLESS

Received February 17, 1982

In this study the binding of amino acids to hexahydrated Cu^{2+} and Ni^{2+} ions, a process presumed to occur when they are adsorbed in the interlamellar space of homoionic smectite clays, has been characterized by using a semiempirical molecular orbital method. For the investigation of both metal ion and amino acid specificity in binding, five α-amino acids, α-alanine, valine, sarcosine, α-aminobutyric acid, and α-aminoisobutyric acid, as well as β-alanine and γ-aminobutyric acid were included. The α-, β-, and γ-amino acids were assumed to bind as bidentate anionic ligands, forming either 1:1 or 1:2 six-coordinated five-, six-, and seven-membered-ring chelate complexes, respectively. Energies of complex formation, optimized geometries, and electron and spin distributions were obtained; and steric constraints of binding of the amino acids to the ion-exchanged cations in the interlamellar spacing of a clay were examined. The results of these studies suggest that hexahydrated Cu^{2+} forms more stable complexes than hexahydrated Ni^{2+} with all the amino acids studied. Among these amino acids, complex formation does not favor the adsorption of the biological subset. Calculated energetics of complex formation and steric constraints predict that 1:1 rather than 1:2 metal-amino acid complexes are generally favored in the clay. Calculated spin densities for these two types of complexes suggest that electron spin resonance techniques can be used to further verify this prediction.

Introduction

It has been proposed that a crucial step in the origin of life was the formation of important biopolymers from the simple organic molecules contained in the primitive atmosphere. Among many aspects of prebiotic synthesis under consideration is the possible prebiological role of clay surfaces, first suggested by Bernal,[1] in processes such as selection and concentration of key monomers from dilute aqueous solution and their subsequent condensation to bipolymers.[2-11] In particular, the

---

* To whom all correspondence should be addressed at the Molecular Research Institute.

(1) Bernal, J. D. "The Physical Basis of Life"; Routledge and Kegan Paul: London, 1951.

(2) Paecht-Horowitz, M.; Berger, J.; Katchalsky, A. *Nature (London)* **1970**, *228*, 636.

0020-1669/83/1322-0111$01.50/0

mechanism of selection and condensation of only 20 L-α-amino acids from dilute solution to form oligomers and proteins initiated by clays has been an important subject of investigation in the realm of chemical evolution of life.

The adsorption properties of clay surfaces are sensitive to pH conditions, the nature of exchangeable metal ion, the degree of hydration, and/or the size and nature of the adsorbate. Specifically, the important biomonomers such as amino acids and nucleotides are not readily adsorbed on the naturally occurring clays that contain alkali and alkaline earth exchangeable cations at nearly neutral pH conditions, thought to have existed in the primitive ocean. However, clays containing the divalent ions as the exchangeable cation have been shown to adsorb amino acids[11,12] and nucleotides[13] at nearly neutral pH. These results imply that the coordination complex formation between the transition metal ion and the electron-donating adsorbates (ligands) is an important interaction in adsorption.

Detailed experimental studies[13] using Zn^{2+}, Cu^{2+}, Ni^{2+}, Co^{2+}, and Mg^{2+} homoionic smectite clays have demonstrated a significant adsorption of a variety of nucleotides on these clays with both a metal ion and nucleotide specificity, indicative of direct interaction between metal ions and nucleotides in the adsorption process. Such interactions were the subject of a complementary theoretical study[14] recently made in our laboratory by using an INDO-type semiempirical molecular orbital method[15] to characterize the binding of a series of nucleotides to hydrated Zn^{2+} and Mg^{2+} ions. The calculated energetics of complex formation for different modes of nucleotide–cation binding successfully accounted for the observed specificities, thus demonstrating that complex formation is a plausible mechanism for adsorption of nucleotides by ion-exchanged clays.

Preliminary experiments at NASA-Ames,[16] similar to those performed for nucleotides, have been carried out for the adsorption of amino acids from a dilute (10^{-4} M) solution of a mixture of amino acids on homoionic smectite clays. These preliminary experiments indicated that the percent of amino acid adsorbed from solution decreased in the order $Cu^{2+} > Ni^{2+} > Zn^{2+} > Na^{+}$. There was also some indication that the subset of amino acids found in proteins would be preferentially adsorbed on the homionic clays.

In a parallel study, we have characterized the stability and electronic structure of complexes formed between Cu^{2+} and Ni^{2+} and selected amino acids under conditions that could mimic the adsorption of amino acids by ion-exchanged hydrated cations in the interlamallar layer of smectite clays. Our major goal was to ascertain the type of amino acid and cation specificity predicted by the thermodynamics of complex formation under such conditions. For the investigation of metal ion specificity in the adsorption process, the two metal ions Cu^{2+} and Ni^{2+}, which were most effective in adsorbing amino acids onto homoionic smectite clays, were chosen. For the investigation of possible amino acid selectivity, the seven amino acids shown in Figure 1 were chosen for study. Among the five α-amino acids chosen were α-alanine (α-Ala) and valine (Val), which occur in proteins, and sarcosine (Sar), α-aminobutyric acid (Aba), and α-aminoisobutyric acid (Aaib), which do not. In addition, for comparison of the behavior of different classes of amino acids, β-alanine (β-Ala) and γ-aminobutyric acid (Gaba) were also included.

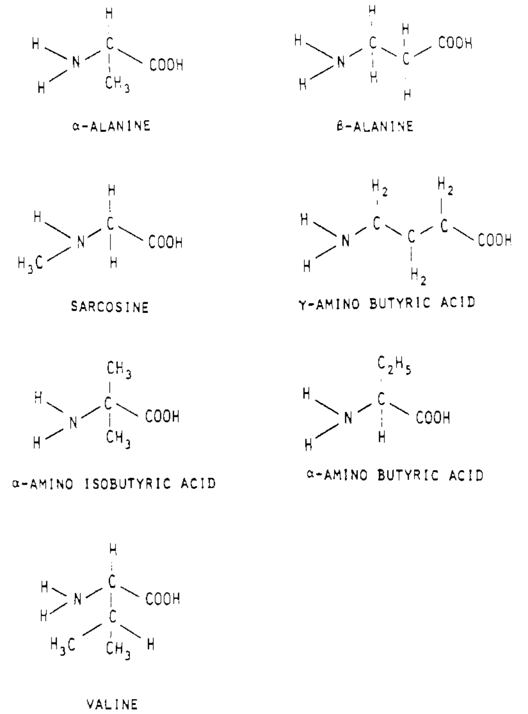

α-ALANINE

β-ALANINE

SARCOSINE

γ-AMINO BUTYRIC ACID

α-AMINO ISOBUTYRIC ACID

α-AMINO BUTYRIC ACID

VALINE

Figure 1. Schematic structures of the seven amino acids investigated.

In the model of cation–amino acid complex formation used here, which could be relevant for the interlamellar layer of smectite clays, we have utilized diverse experimental observations. Although we have not explicitly included the direct electronic effects of the clay environment on the complex formation, steric effects of such complex formation have been examined and a number of other important features of complex formation that are unique to the clay environment, as distinguished from bulk solvent, have been included.

The stability of transition-metal amino acid complexes in solution has been extensively investigated, and a number of crystal structures have been determined. These studies indicated the following features of complex formation in solution:

(1) Complex formation occurs with the anionic form of the amino acid, even though the zwitterionic form predominates.

(2) 1:2 metal–amino acid complexes are more stable than 1:1, and the hexacoordinated complex, with two H_2O's of hydration, is obtained in most crystal structures.

(3) As revealed by X-ray crystal structure determinations, complex formation of amino acids is always of a chelate form with the anionic carboxyl oxygen and neutral amine nitrogen directly coordinated to the metal.

Amino acid complexing to transition metals in the exchangeable cationic sites of smectite clays share some of these characteristics but differ in others.

Most experimental work is being carried out with dilute solutions of single amino acids and Wyoming smectite, a dioctahedral, three-layer, 2:1 silicon–aluminum clay. The description of the clay tactoid is shown schematically in Figure 2. Under the experimental conditions, the exchangeable Cu^{2+} and Ni^{2+} ions in the interlamellar space of clay are believed to be fully hydrated, forming hexahydrated complexes as ev-

---

(3) Paecht-Horowitz, M. *Isr. J. Chem.* **1973**, *11*, 369.
(4) Cairns-Smith, A. G. *Proc. R. Soc. London, Ser. B* **1975**, *189*, 249.
(5) Otroschenko, V. A.; Vasilyeva, N. V. *Origin Life* **1977**, *8*, 25.
(6) Friebele, E.; Shimoyama, A.; Ponnamperuma, C. *J. Mol. Evol.* **1980**, *16*, 269.
(7) Theng, B. K. G. "The Chemistry of Clay-Organic Reactions"; Wiley: New York, 1974.
(8) Lahav, N.; Chang, S. *J. Mol. Evol.* **1976**, *8*, 357.
(9) Lahav, N.; White, D.; Chang, S. *Science (Washington, D.C.)* **1978**, *201*, 67.
(10) Lahav, N; White, D. *J. Mol. Evol.* **1980**, *16*, 11.
(11) Jang, S. D. Ph.D. Thesis, State University of New York, 1977.
(12) Lawless, J. G.; Levi, N. *J. Mol. Vol.* **1979**, *13*, 281.
(13) Lawless, J. G.; Edleson, E. G. "Life Sciences and Space Research"; Pergamon Press: New York, 1980; Vol. VIII, pp 81–88.
(14) Liebmann, P.; Loew, G.; Burt, S.; Lawless, J.; MacElroy, R. D. *Inorg. Chem.* **1982**, *21*, 1586.
(15) Zerner, M.; Loew, G. H.; Kirchner, R. F.; Muller-Westerhoff, U. T. *J. Am. Chem. Soc.* **1980**, *102*, 589.
(16) Lawless, J. G., unpublished experimental results.

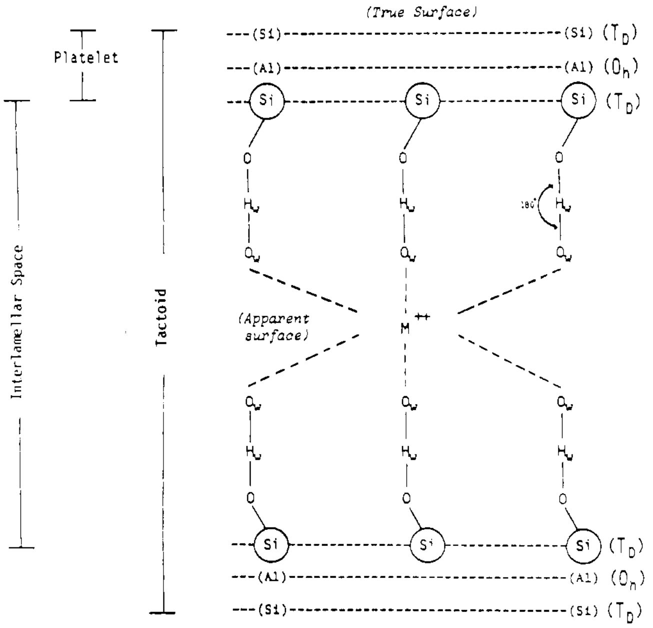

Figure 2. Schematic structure of a repeating tactoid unit of a vermiculite clay.

idenced by ESR studies of Cu^{2+}–clay systems.[17] Nevertheless, complex formation in the clays takes place under limited hydration conditions compared to the case in bulk water.

Infrared studies by Jang[12] of amino acids adsorbed on homoionic montmorillonites in the pH range 3–9 provide evidence of chelate ring formation at equilibrium pH values greater than 6. However, in contrast to the situation without clay, a concomitant drop in pH of the solution containing clay suspension and amino acid is also observed, providing evidence that complex formation occurs by the release of a proton from the zwitterionic form of the amino acid. Thus, one major difference between complex formation in solution and in the clay, incorporated in our model, is the energy required to form an anionic form of the amino acid from the zwitterionic form that is adsorbed in the clay. Another possible difference that has been suggested is that formation of 1:1 metal–amino acid complexes is favored in the clay.[12]

To incorporate some of the differences between solution and clay behavior, in this study, we considered both 1:1 and 1:2, partially hydrated, six-coordinated metal–amino acid complexes to be formed from both the anionic and zwitterionic forms of the amino acids and hexahydrated metal ions. Optimized geometries, energies, electron distributions, and spin distributions were obtained for reactants and products, together with the energies of complex formation. Using computer graphics, we also examined steric constraints of binding the amino acids to the ion-exchanged hydrated cation in the interlamellar spacing of the clay.

The results of these studies yield for the first time a detailed stereoelectronic description of metal–amino acid complexes, which up to now have been considered only in the framework of more approximate, qualitative theories. They also lead to predictions of both cation and amino acid specificities in extent of adsorption and of the stoichiometry of the complex in the clay.

Electron spin resonance spectra of cation–amino acid complexes in clay systems are suggested to further verify predictions made about the stoichiometry of the metal–ligand binding in these complexes.

Models and Assumptions

Consistent with the observations discussed above and the experimental conditions employed, i.e., clays suspended in dilute solutions of amino acids at neutral pH, the following model was assumed in this study of transition metal–amino acid complex formation, which should be relevant to conditions in the interlamellar layer of the clay: (1) Complex formation occurs between a hexahydrated metal cation and the zwitterionic form of the amino acid. (2) Both the carboxyl oxygen and amine nitrogen of the amino acid bind directly to the metal with the loss of a proton from the amine nitrogen, leaving the anionic form of the amino acid as a bidentate chelated ligand in the complex. (3) In this bidentate mode of binding, each amino acid anion displacing two H_2O's of hydration of the metal. (4) Metal ion complexes with both one and two amino acids were considered. (5) Each metal ion in its complex has a coordination number of 6 with approximately octahedral symmetry.[18]

With this model and assumptions, the energetics (ΔE_R) of complex formation could be calculated from the reaction

$$M(H_2O)_6^{2+} + nAAZI \overset{\Delta E_R}{\rightleftharpoons} [M(AAA^-)_n(H_2O)_{6-2n}]^{(2-n)+} + nH_3O^+ + nH_2O \quad (1)$$

where M is Cu or Ni, AAZI is the zwitterionic form of amino acid, AAA^- is the anionic form of amino acid, and n is the number of moles of amino acids that form a complex with 1 mol of metal cation. The ground state of each six-coordinated Cu^{2+}–amino acid complex is a doublet state, and each Ni^{2+}–amino acid complex is assumed to retain a triplet ground state as in the hexahydrated complex.

While it is possible to envisage that the adsorption of amino acids into the interlamellar region of clays may involve direct interaction between the silicate framework and the amino acids, most experimental evidence indicates that direct intereaction occurs between the hydrated transition metal and the zwitterionic form of amino acids.[7,12] Thus the energetics of reaction 1 could be a dominant feature in determining the efficacy and selectivity of various cationic exchanged clays in adsorbing amino acids, with the clay environment itself providing a media for interactions involving the zwitterion free from bulk water.

By contrast, the bulk water, the predominant interaction between amino acids and transition metals is known to occur directly with the anionic form of the amino acids, and the solution equilibrium constants reported are based on the equilibrium expression[19]

$$M(H_2O)_6^{2+} + nAAA^- \rightarrow M(AAA)_n(H_2O)_{6-2n}^{(2-n)+} + 2nH_2O \quad (2)$$

where AAA^- is the anionic form of amino acid and n is the number of moles of amino acids binding to the metals. Thus, in the results presented here, this equation has been used to calculate the energetics of 1:1 and 1:2 complex formation in order to compare them with observed stability constants in solution. Differences in calculated energetics obtained between processes 1 and 2 can then be related to possible differences in complex formation in homoionic clays compared to known complex formation in solution. Explicit interactions between the complexes hydrated cation and the adjacent silicate layers in the interlamellar region of the clay were, however, not considered.

The steric constraints of binding the amino acids to the ion-exchanged hydrated cation in the interlamellar spacing

---

(17) Pinnavaia, T. J. "Advanced Chemical Methods for Soil and and Clay Mineral Research"; Stucki, J. W., Banwart, W. L., Eds.; D. Reidel: Boston, 1980, Vol. 63, pp 391–419.

(18) Anglici, R. J. "Inorganic Biochemistry"; Eichhorn, G. L., Ed.; Elsevier: New York, 1973; Vol. 1, pp 63–101.

(19) Dobbie, H.; Kermack, W. O.; Lees, H. *Biochem. J.* **1955**, *59*, 240.

Table I. Calculated Energy of Reaction (ΔE_R, kcal/mol) for Metal–Amino Acid Complex Formation by the Equation

$$\mathrm{M(H_2O)_6}^{2+} + n\mathrm{AAZI} \overset{\Delta E_R}{\rightleftharpoons} [\mathrm{M(AAA^-)}_n\mathrm{(H_2O)}_{6-2n}]^{(2-n)+} + n\mathrm{H_2O} + n\mathrm{H_3O}^{+\,a}$$

	crystal or composite geometries				optimized geometries			
	$n = 1$ (1:1)		$n = 2$ (1:2)		$n = 1$ (1:1)		$n = 2$ (1:2)	
amino acid	Cu	Ni	Cu	Ni	Cu	Ni	Cu	Ni
α-Ala[b]	−143.5	−113.0	−127.4	−108.8	−108.4	−87.6	−55.5	−41.8
Sar[b]	−137.1	−106.2	−114.1	−95.1	−115.4	−93.5	−46.4	−47.9
Aba[b]	−132.1	−101.8	−103.9	−85.3	−108.4	−88.3	+1.0	−42.6
Aaib[b]	−132.4	−101.5	−102.7	−84.0	−126.0	−101.9	−73.5	−51.4
Val[b]	−119.2	−88.5	−76.6	−57.8	−104.8	−84.4	−47.8	−34.4
β-Ala[b]	−120.1	−85.2	−119.6	−108.0	*c*	−149.2	*c*	−97.4
Gaba[b]	−213.4	−190.5	−246.9	−230.0	−197.9	−190.3	−134.6	−115.7

[a] M = metal ion; AAZI = zwitterionic form of amino acid; AAA$^-$ = anionic form of amino acid. [b] Abbreviations: α-Ala, α-alanine; Sar, sarcosine; Aba, α-aminobutyric acid; Aaib, α-aminoisobutyric acid; Val, valine; β-Ala, β-alanine; Gaba, γ-aminobutyric acid. [c] Starting with a crystal or composite geometry for this complex optimization procedure failed to calculate an optimized geometry within the convergence criteria used to identify a minimum.

(~10.8 Å) of the clay were examined with use of a fixed interlamellar spacing. Generally, the interlamellar spacing depends on the extent of hydration and the nature and concentration of the adsorbates. However, under fully hydrated conditions the addition of low concentration of amino acid should not alter this spacing significantly.

Method and Procedure

In this study, an INDO-type[15] semiempirical molecular orbital method was used, which includes transition-metal atoms and total geometry optimization to compute the energies, optimized geometries, and electronic structure of hydrated cations, amino acids, and all the metal–amino acid complexes studied. Since the Cu^{2+} complexes are doublets with one unpaired spin and the Ni^{2+} complexes are assumed to be triplet states with two unpaired spins, the UHF-SCF (unrestricted Hartree–Fock self-consistent field) procedure was used for all calculations involving the transition-metal complexes. Crystal structure data were used for α-alanine,[20] β-alanine,[21] and Gaba,[22] and composite structures based on that for α-alanine were used for sarcosine, Aba, Aaib, and valine as input geometries. Crystal structure data were also used for initial geometries of hexahydrated Ni^{2+}[23] and Cu^{2+}.[24] The initial geometry of all five-membered-ring and metal–α-amino acid complexes was taken from the crystal structure of bis(α-alanine)copper(II),[25] and that for the six-membered-ring chelate complexes from the structure of bis(β-alanine)copper(II)[26] and -nickel(II)[27] complexes. While the crystal structure of sarcosine, Aba, valine, and the bis complex $\mathrm{Cu^{II}(Aba)_2}$[28] have been reported, these are not significantly different from the composite geometries selected, which had the advantage of supplying more uniform starting geometries for all the α-amino acids studied.

In the absence of a crystal structure for M^{2+}–Gaba complexes, which can form seven-membered chelate rings, the initial geometry selected was based on known bond angles and bond distances of Gaba. Values of torsion angles were selected such that the chelating atoms N and O were about 2.0 Å away from the central metal ion and the bond angle N–M–O was close to 90°.

The two equatorial water molecules, in the six-coordinated 1:1 complexes, or the ligands of the second amino acid, in 1:2 complexes, were oriented in such a way that the four atoms bonded to the central metal ion in xy plane were along the $\pm x$ and $\pm y$ axes, i.e., pointing toward the lobes of the $d_{x^2-y^2}$ orbital of the transition metal cation. A trans arrangement of N and O atom ligands around the central metal ion was chosen for the 1:2 complexes. Crystal structures of hydrated Cu^{2+} and Ni^{2+} complexes reveal a systematic difference between them—in that the Cu bond distances to axial $\mathrm{H_2O}$ ligands are significantly longer, with a greater resulting tetragonal distortion. Optimization of the M–$\mathrm{H_2O}$ distance for 1:1 complexes (α-alanine)copper(II) (2.1 Å) and (α-alanine)nickel(II) (2.0 Å) eliminated most of this difference. These values were used as part of the input geometries of all the M^+–amino acid complexes.

Total geometry optimization was carried out for the hydrated metal ions, all the amino acid anions, and the six-coordinated 1:1 metal–amino acid complexes. The optimized geometries of the amino acid anions were used to calculate the zwitterion energy. This process was adopted because direct optimization of the zwitterion yielded the neutral form of the amino acids. Also, the optimized geometries of the 1:1 complexes were used to construct and calculate single-point energies for the 1:2 complexes, with the second amino acid assumed to form a chelate ring identical with the first, a reasonable assumption for identical ligands.

Results

A. Energetics of Complex Formation with Zwitterionic Amino Acids. The calculated energies of formation (ΔE_R) of 1:1 complexes with Cu^{2+} and Ni^{2+} in the adsorption process depicted by reaction 1 are given in Table I for the seven amino acids studied. These results show that, in general, the chelation process assumed to occur in the clay is energetically more favored with Cu^{2+} than with Ni^{2+}. Among the seven amino acids studied, these calculations predict that Gaba complexes, whiich form a seven-membered chelate ring, are most favored. The order of stability of the remaining amino acid complexes depends to some extent on the geometries employed for the reactants and products. When nonoptimized crystal or composite geometries of $\mathrm{H_2O}$, $\mathrm{H_3O^+}$, amino acids, hexahydrated Cu^{2+} and Ni^{2+}, and metal–amino acid complexes are used, the relative preference of the α-amino acids to form five-membered chelate complexes is in the order α-Ala > Sar > Aba ≃ Aaib > Val, with β-Ala, which forms a six-membered-ring complex, found to be about equal in stability to or somewhat less stable than Val. However, this order of specificity changes if totally optimized geometries are used. From optimized geometries of reactants and products, the calculated order of extent of complex formation with Cu^{2+} is Gaba > Aaib > Sar > Aba = α-Ala > Val; with Ni^{2+} the order is Gaba > β-Ala > Aaib > Sar > Aba ≃ α-Ala > Val.

The energetics of formation of 1:2 metal–amino acid complexes by the process assumed to occur in the clay were also calculated (eq 1) with use of crystal or composite geometries and optimized geometries of reactants and products as described under Method and Procedure. The resultant energies

---

(20) Lehmann, M. S.; Koetzle, T. F.; Hamilton, W. C. *J. Am. Chem. Soc.* **1972**, *94*, 2657.

(21) Jose, P.; Pant, L. M. *Acta Crystallogr.* **1965**, *18*, 806.

(22) Steward, E. G.; Player, R. B.; Warner, D. *Acta Crystallogr., Sect. B* **1973**, *B29*, 2038.

(23) Biogoli, F.; Braibanti, A.; Tiripicchio, A.; Camellini, M. T. *Acta Crystallogr., Sect. B* **1971**, *B27*, 1427.

(24) Montgomery, H.; Lingafelter, E. C. *Acta Crystallogr.* **1966**, *20*, 659.

(25) Dijkstra, A. *Acta Crystallogr.* **1966**, *20*, 588.

(26) Mitsui, Y.; Iitaka, Y.; Sakaguchi, H. *Acta Crystallogr.*, **1974**, *B32*, 1634.

(27) Jose, P.; Pant, L. M.; Biswas, A. B. *Acta Crystallogr.* **1964**, *17*, 24.

(28) Fawcett, T. G.; Ushay, M.; Rose, J. P.; Lalancette, R. A.; Potenza, J. A.; Schugar, H. J. *Inorg. Chem.* **1979**, *18*, 327.

Table II. Calculated Energy of Reaction (ΔE_R, kcal/mol) for Metal–Amino Acid Complex Formation by the Equation

$$M(H_2O)_6^{2+} + nAAA^- \overset{\Delta E_R}{\rightleftharpoons} [M(AAA^-)_n(H_2O)_{6-2n}]^{(2-n)+} + 2nH_2O^a$$

	crystal or composite geometries				optimized geometries			
	$n = 1$ (1:1)		$n = 2$ (1:2)		$n = 1$ (1:1)		$n = 2$ (1:2)	
amino acid	Cu	Ni	Cu	Ni	Cu	Ni	Cu	Ni
α-Ala[b]	−325.3	−294.8	−491.1	−472.4	−275.8	−254.9	−390.1	−376.5
Sar[b]	−318.2	−287.3	−476.3	−457.3	−271.8	−249.9	−359.3	−360.7
Aba[b]	−314.1	−283.8	−468.0	−449.3	−276.3	−256.2	−334.7	−378.3
Aaib[b]	−315.4	−284.6	−468.9	−450.2	−294.6	−270.5	−410.8	−388.7
Val[b]	−301.8	−271.1	−441.9	−423.1	−262.7	−242.3	−363.7	−350.4
β-Ala[b]	−286.4	−251.6	−450.7	−452.3	*c*	−307.3	*c*	−393.5
Gaba[b]	−360.1	−337.2	−540.3	−523.4	−330.9	−323.2	−400.3	−381.4

[a] M = metal ion; AAA^- = anionic form of amino acid. [b] The abbreviations for amino acids are the same as in Table I. [c] See footnote *c* of Table I.

of reaction, ΔE_R, are also given in Table I. As in the 1:1 complexes, Cu^{2+} is predicted to be more effective in adsorption of all the amino acids, and the order of stability of complex formation by the amino acids is somewhat different when nonoptimized and optimized geometries are used.

B. Energetics of Complex Formation with Anionic Amino Acids. The energetics of 1:1 and 1:2 complex formation using reaction 2, corresponding to the solution reaction, are summarized in Table II. For crystal structure geometries, the order of stability of 1:1 complexes formed by Cu^{2+} and Ni^{2+} is Gaba > α-Ala > Sar > Aaib ~ Aba > Val > β-Ala, while for 1:2 complexes β-Ala becomes somewhat more stable than Val. As seen in Table II, this order of stability is again altered by geometry optimization.

C. Geometries of Complexes. The optimized geometries of 1:1 complexes of α-Ala with Cu^{2+} and Ni^{2+} are shown in Figure 3. As shown in this figure, both metals have essentially square-planar bonding. The in-plane bond angles deviate only slightly from 90°, and metal–ligand bond lengths are somewhat unequal with the M–carbonyl oxygen bond the shortest. The five-membered chelate ring is nearly planar, but with a small amount of puckering around the C_α atom. This puckering is least for α-aminoisobutyric acid, which has two CH_3 groups on the C_α carbon and forms a planar chelate ring. This planarity enhances the relative stability of this complex, making it the most favored of the α-amino acids (Table I).

The effect of total geometry optimization is more profound for the six-membered ring formed by β-alanine with Cu^{2+} and Ni^{2+}. There is more flexibility in the ring structure, and it rearranges from the crystal structure to allow intramolecular interaction between an axial H_2O and the carbonyl oxygen of the β-amino acid. Such an optimized structure is shown in Figure 4b for the 1:1 Ni^{II}(β-Ala)·$4H_2O$ complex. The CO···HOH distance is 1.17 Å, indicating significant intramolecular interaction. While such a configuration most likely exists for the Cu^{2+} complex as well, we could not obtain a totally converged geometry starting from the crystal structure of Cu^{II}(β-Ala), which has multiple intermolecular interactions.

Optimized geometries of Cu^{II}(Gaba)·$4H_2O$ and Ni^{II}(Gaba)·$4H_2O$ complexes are shown in Figure 5. As seen in this figure, the seven-membered rings are in the form of a half-chair with the O–Cu–N–C_γ atoms in a plane perpendicular to C_0–C_α–C_β–C_γ plane. As in the six-membered-ring complex formed by β-alanine, the carbonyl oxygen has significant intermolecular interaction with the hydrogen of an axial H_2O molecule.

D. Steric Considerations. To examine the steric consequences of binding of amino acids to cations at the exchangeable site of homoionic smectite clays, we have used a crystal structure of a vermiculite clay with a hexahydrated Mg^{2+} ion at the exchangeable cationic site in the interlamellar layer.[29] We have used this clay structure in a similar fashion in our previous studies to examine the steric consequences of nucleotide complex formation. The portion of the clay used is shown in Figure 6, consisting of a single unit of two T_d silicate layers ($Si_6O_{18}H_{12}$) representing the boundaries of the interlamellar spacing. In this spacing the hexahydrated cation is surrounded by six H_2O molecules as it is in the crystal structure. The general structure of this vermiculite should be a reasonable enough approximation to the smectite used in the experiments for adsorption of amino acid from aqueous solution to be used to examine steric consequences of amino acid complex formation.

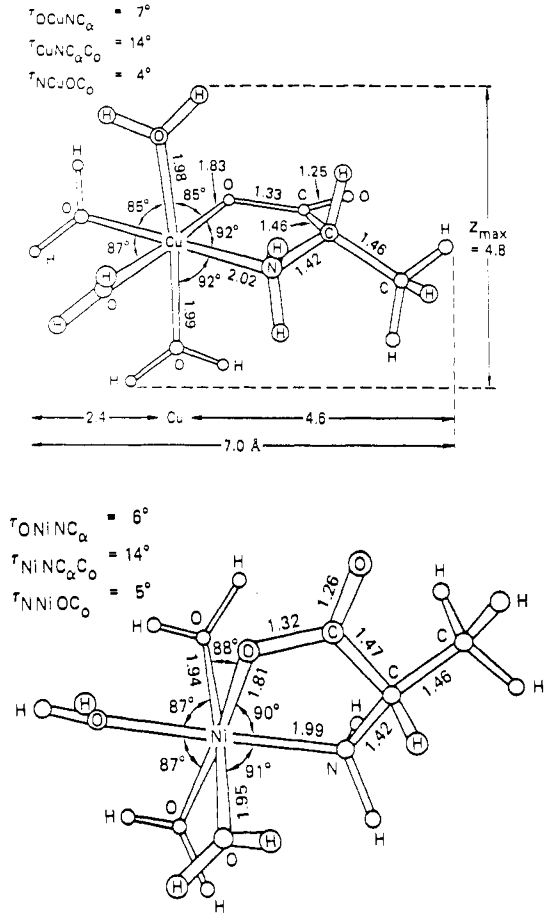

Figure 3. Optimized geometries of 1:1 coordinated metal–α-amino acid complexes: (a) (top) Cu^{II}(α-Ala)·$4H_2O$; (b) (bottom) Ni^{II}(α-Ala)·$4H_2O$.

---

[29] Mathieson, A. M. *Am. Mineral.* **1958**, *43*, 216.

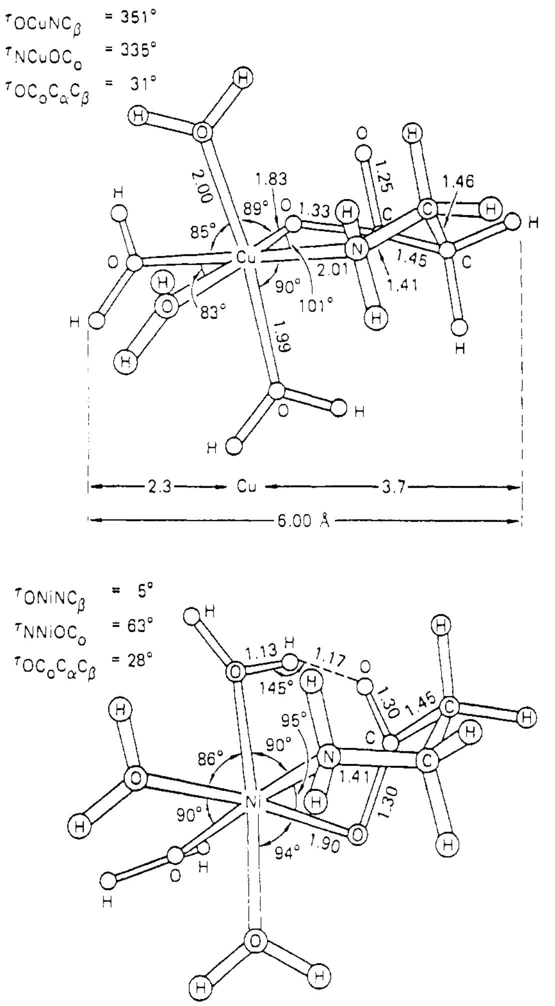

Figure 4. Geometries of 1:1 coordinated metal–β-amino acid complexes: (a) (top) $Cu^{II}(\beta\text{-Ala})\cdot 4H_2O$ (not optimized); (b) (bottom) $Ni^{II}(\beta\text{-Ala})\cdot 4H_2O$ (optimized).

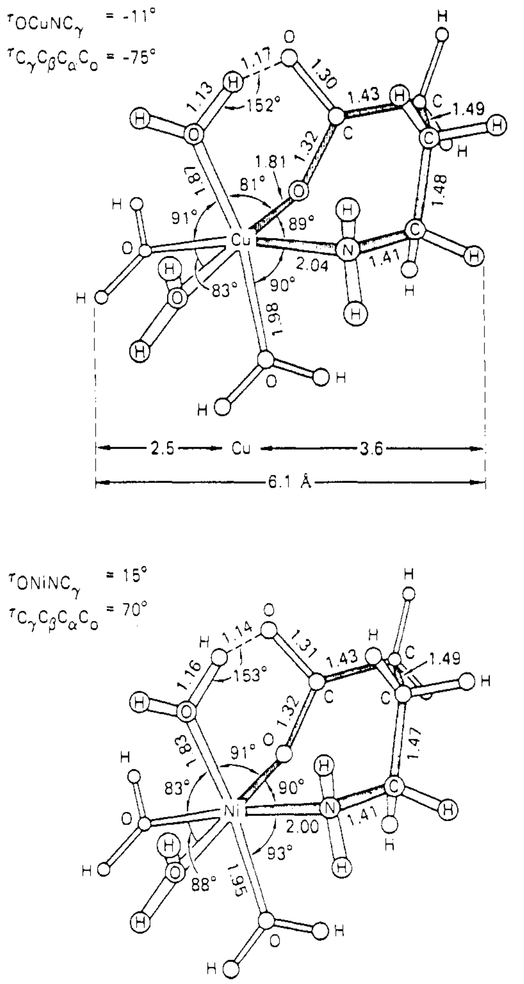

Figure 5. Optimized geometries of 1:1 six-coordinated metal–γ-amino acid complexes: (a) (top) Cu^{2+}–γ-amino acid complexes; (b) (bottom) Ni^{2+}–γ-amino acid complexes.

Figures 7–9 show the interlamellar space in which the metal ion, at its exchangeable site, has formed a 1:1 complex with α-Ala, β-Ala, and Gaba while retaining four H_2O's of hydration. These figures were obtained by inserting the geometry-optimized complexes into the crystal structure of the clay with the Cu^{2+} and Ni^{2+} ions taking the place of the Mg^{2+}. Figures 7 and 8 indicate that within the steric constraints in the interlamellar spacing both α- and β-amino acids can form complexes with the metal ion. These complexes could be rotated around the cation to a position that eliminated repulsive interaction with the two silicate layers. In addition, as shown in these figures, H bonding between the bound H_2O molecules and the silicate oxygens is retained in complex formation.

By contrast, in the seven-membered-ring chelate formed by the γ-amino acid, as shown in Figure 9, there is close (~2 Å) contact between the free carbonyl oxygen and two silicate oxygens of the clay. No rotation could be found to avoid such contact with at least one silicate oxygen. Since the 2-Å distance obtained is much smaller than the van der Waals radii of two oxygen atoms (~3 Å), the resultant repulsion decreases the likelihood of γ-amino acid chelate complex formation with exchangeable cations in homoionic smectite clays, despite its favorable energetics.

The ion-exchangeable sites have been estimated to be ~10 Å apart.[30] As indicated in Figures 3 and 4, the bare nuclei to nuclei maximum dimension of a 1:2 M–α-Ala complex would be ~9.2 Å and for a M–β-Ala complex ~7.4 Å. If the van der Waals radii of 1.2 Å for two hydrogen atoms are taken into account, 1:2 complexes of α-Ala (and α-amino acids in general) would not fit between metal sites, while M–β-Ala complexes would fit.

E. Electronic Structure. In addition to the energetics and geometry of complex formation, the electron and spin distribution in the complexes and their variation with metal ion and stoichiometry have been calculated. Tables III–VI give the calculated net charges, bond overlaps, and atomic orbital populations in 1:1 and 1:2 metal–amino acid complexes and, for comparison, those in the hexahydrated metal complexes.

The metal and ligand orbitals with significant spin density, i.e., radical character, are given in Table VII. These orbital spin densities were calculated as the difference in α- and β-electron densities corrected for spin contamination from higher spin states.

Discussion

The calculated energetics of complex formation indicates that, in general, Cu^{2+} forms more stable complexes than Ni^{2+} with both the zwitterionic and anionic forms of amino acids. Thus the extent of adsorption of amino acids by Cu^{2+} is predicted to be greater than for Ni^{2+}-exchanged homoionic clays, consistent with the preliminary work carried out at NASA-Ames and also with the Irving–Williams order of complex stabilities.[31]

---

[30] Van Olphen, H. "An Introduction to Clay Colloid Chemistry", 2nd ed.; Wiley: New York, 1977; pp 254–255.

[31] Basolo, F; Pearson, R. G. "Mechanisms of Inorganic Reactions"; Wiley: New York, 1967; p 77.

Table III. Calculated Electron Distribution in 1:1 Metal (M)-Amino Acid Complexes

	M = Cu					M = Ni				
	q_{Cu}[a]	Σq_{H_2O}[b]	Σq_{AAA}[c]	ρ_{M-O}[d]	ρ_{M-N}[e]	q_{Ni}[a]	Σq_{H_2O}[b]	Σq_{AAA}[c]	ρ_{M-O}[d]	ρ_{M-N}[e]
M^{2+}	2.00+					2.0+				
$M(H_2O)_6^{2+}$	0.92+	0.18+				0.93+	0.178+			
M-α-Ala[f]	0.60+	0.12+	0.09−	0.116	0.246	0.81+	0.140+	0.36−	0.351	0.256
M-Sar[f]	0.63+	0.12+	0.11−	0.094	0.265	0.85+	0.140+	0.39−	0.349	0.275
M-Aba[f]	0.60+	0.12+	0.09−	0.120	0.254	0.81+	0.140+	0.36−	0.348	0.256
M-Aaib[f]	0.57+	0.12+	0.04−	0.096	0.235	0.81+	0.140+	0.35−	0.347	0.248
M-Val[f]	0.60+	0.12+	0.09−	0.123	0.257	0.81+	0.140+	0.36−	0.347	0.260
M-Ala[f]	0.57+	0.12+	0.04−	0.137	0.245	0.89+	0.114+	0.34−	0.219	0.215
M-Gaba[f]	0.75+	0.10+	0.16−	0.226	0.184	0.85+	0.103+	0.26−	0.299	0.175

[a] Net charge on the metal ion calculated from Mulliken population analysis. [b] Net average charge on each water molecule coordinated to the metal ion. [c] Net charge on amino acid anion coordinated to the metal ion. [d] Calculated bond-overlap density of metal ion and chelated oxygen of amino acid; this is a measure of bond strength. [e] Calculated bond-overlap density of metal ion and chelated nitrogen of amino acid. [f] The abbreviations for amino acids are the same as in Table I.

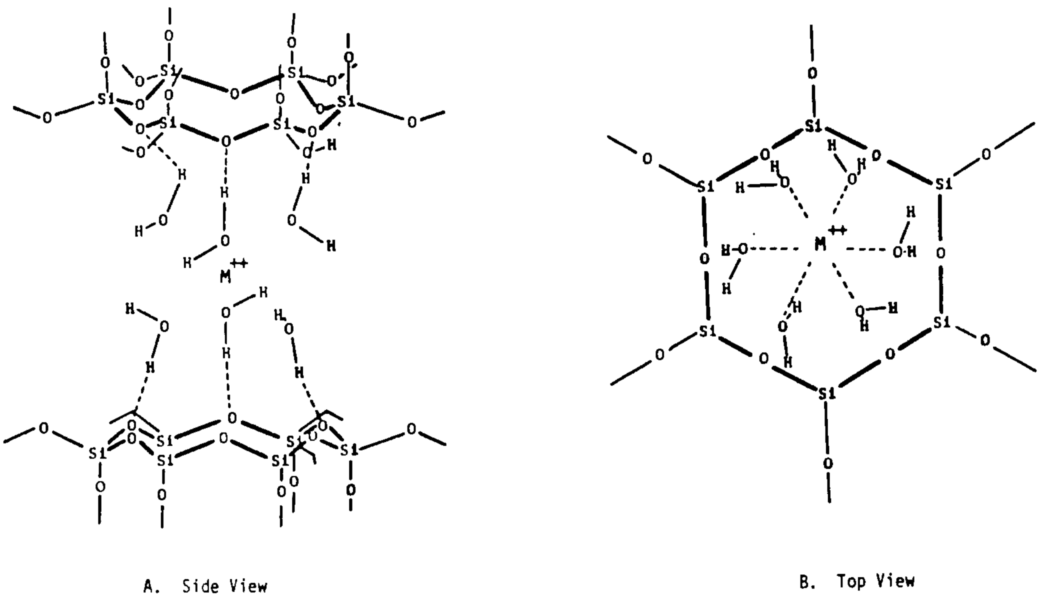

A. Side View

B. Top View

Figure 6. Two units of the silicate layer and a hydrated exchangeable cation (Mg^{2+}) in the interlamellar spacing of a vermiculite clay from X-ray structure.

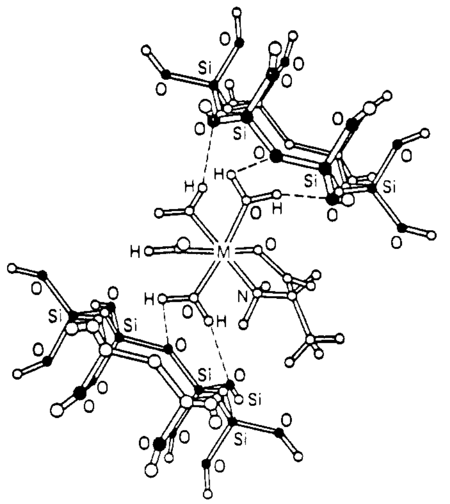

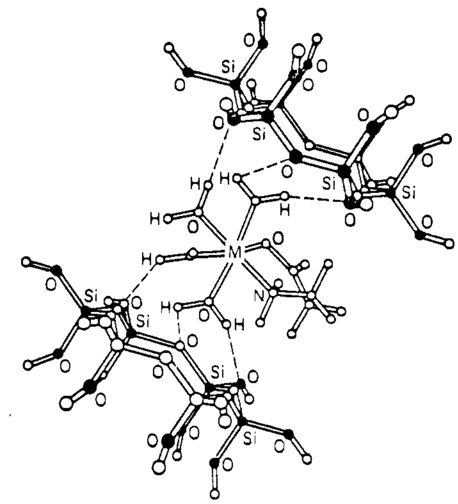

Figure 7. Cu^{II}(α-Ala) in the interlamellar spacing of clay. In this figure, the X-ray structure of clay shown in Figure 6 was used and $Mg^{2+}\cdot 6H_2O$ was replaced in the interlamellar space by the geometry-optimized 1:1 Cu^{II}(α-Ala)$\cdot 4H_2O$ complex with Cu^{2+} replacing Mg^{2+} at the exchangeable cationic site.

Figure 8. Cu(β-Ala) in the interlamellar spacing of a clay. In this figure, the X-ray structure of clay shown in Figure 6 was used and $Mg^{2+}\cdot 6H_2O$ was replaced in the interlamellar space by the 1:1 Cu^{II}(β-Ala)$\cdot 4H_2O$ complex with Cu^{2+} replacing Mg^{2+} at the exchangeable cationic site.

Another significant result is that different energetics of complex formation are predicted depending on whether the transition metal interacts with the zwitterionic form or the anionic form of amino acids.

The formation of the 1:1 complexes by transition metals directly with the anionic form of amino acids is more exothermic than the corresponding complex formation by direct metal ion interaction with the zwitterionic form. This energy

Table IV. Calculated Electron Distribution in 1:2 Metal (M)-Amino Acid Complexes

	M = Cu					M = Ni				
amino acid	q_{Cu}[a]	$\Sigma q_{\mathrm{H_2O}}$[b]	Σq_{AAA}[c]	$\rho_{\mathrm{M-O}}$[d]	$\rho_{\mathrm{M-N}}$[e]	q_{Ni}[a]	$\Sigma q_{\mathrm{H_2O}}$[b]	Σq_{AAA}[c]	$\rho_{\mathrm{M-O}}$[d]	$\rho_{\mathrm{M-N}}$[e]
α-Ala[f]	0.745+	0.084+	0.456−	0.288	0.178	0.849+	0.096+	0.521−	0.327	0.167
Sar[f]	0.819+	0.087+	0.497−	0.293	0.181	0.909+	0.099+	0.554−	0.330	0.175
Aba[f]	0.732+	0.077+	0.443−	0.299	0.186	0.847+	0.096+	0.520−	0.326	0.168
Aaib[f]	0.718+	0.084+	0.443−	0.286	0.168	0.843+	0.092+	0.514−	0.336	0.155
Val[f]	0.736+	0.081+	0.449−	0.288	0.183	0.849+	0.096+	0.520−	0.324	0.170
β-Ala[f]	0.751+	0.079+	0.455−	0.298	0.148	0.972+	0.101+	0.584−	0.247	0.156
Gaba[f]	0.810+	0.091+	0.496−	0.253	0.101	0.899+	0.094+	0.543−	0.288	0.109

[a] Net charge on the metal ion calculated from Mulliken population analysis. [b] Net average charge on each water molecule coordinated to the metal ion. [c] Net average charge on each amino acid anion coordinated to the metal ion. [d] Calculated average bond-overlap density of M-O (amino acid) bond. [e] Calculated average bond overlap density of M-N (amino acid) bond. [f] The abbreviations for amino acids are the same as in Table I.

Table V. Mulliken Orbital Populations of the Metal (M) Orbitals in the 1:1 Metal-Amino Acid Complexes

	4s	$4p_x$	$4p_y$	$4p_z$	$3d_{z^2}$	$3d_{x^2-y^2}$	$3d_{xy}$	$3d_{xz}$	$3d_{yz}$
				M = Cu					
$M(H_2O)_6{}^{2+}$	0.3229	0.1871	0.1952	0.2060	1.9607	1.2843	1.9573	1.9689	1.9985
M-α-Ala[a]	0.2729	0.1468	0.1341	0.1666	1.9430	1.7749	1.9881	1.9980	1.9782
M-Sar[a]	0.2547	0.1268	0.1238	0.1625	1.9476	1.7818	1.9940	1.9967	1.9783
M-Aba[a]	0.2771	0.1515	0.1363	0.1677	1.9448	1.7646	1.9868	1.9978	1.9750
M-Aaib[a]	0.2620	0.1405	0.1185	0.1638	1.9440	1.8138	1.9915	1.9977	1.9983
M-Val[a]	0.2787	0.1530	0.1375	0.1683	1.9448	1.7615	1.9835	1.9976	1.9752
M-β-Ala[a]	0.2796	0.1536	0.1397	0.1570	1.9647	1.7784	1.9972	1.9985	1.9628
M-Gaba[a]	0.3187	0.1786	0.1537	0.2092	1.8481	1.5518	1.9894	1.9980	1.9992
				M = Ni					
$M(H_2O)_6{}^{2+}$	0.2923	0.1873	0.1871	0.1868	1.1943	1.1932	1.9451	1.9448	1.9440
M-α-Ala[a]	0.3078	0.1711	0.2108	0.1883	1.1923	1.2670	1.9622	1.9691	1.9198
M-Sar[a]	0.2956	0.1578	0.2018	0.1861	1.1749	1.2559	1.9776	1.9822	1.9222
M-Aba[a]	0.3061	0.1761	0.2068	0.1894	1.1894	1.2662	1.9631	1.9733	1.9216
M-Aaib[a]	0.3091	0.1772	0.2024	0.1872	1.1234	1.2681	1.9459	1.9857	1.9945
M-Val[a]	0.3062	0.1741	0.2083	0.1884	1.1931	1.2740	1.9584	1.9727	1.9124
M-β-Ala[a]	0.2868	0.1781	0.1660	0.2096	1.1857	1.1847	1.9565	1.9660	1.9780
M-Gaba[a]	0.3065	0.1752	0.1844	0.2076	1.1718	1.1706	1.9817	1.9495	1.9987

[a] The abbreviations for amino acids are the same as in Table I.

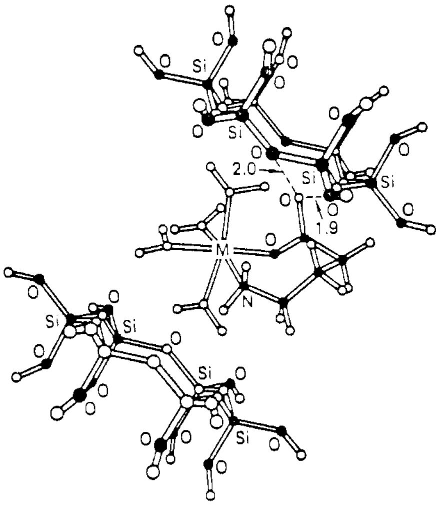

Figure 9. Cu(Gaba) in the interlamellar spacing of a clay. In this figure, the X-ray structure of clay shown in Figure 6 was used and $Mg^{2+}\cdot 6H_2O$ was replaced in the interlamellar space by the geometry-optimized 1:1 $Cu^{II}(Gaba)\cdot 4H_2O$ complex with Cu^{2+} replacing Mg^{2+} at the exchangeable cationic site.

difference reflects the additional energy required to release the proton bound to the amine nitrogen of the zwitterion when it complexes to the metal. The factors contributing to the diminished exothermicity of complex formation with the zwitterion compared to the anionic form of the amino acid also lead to the prediction that only 1:1 complexes will be formed by the zwitterion, while both 1:1 and 1:2 complexes will be formed by the anion. Transition-metal complexes with the zwitterionic form of amino acids are assumed to be occurring in the clay, while complex formation with the anionic form of the amino acid is the basis for the solution equilibrium constants reported.

The result obtained that both 1:1 and 1:2 complexes can be formed by Cu^{2+} and Ni^{2+} with the anionic form of amino acids is consistent with observed solution behavior where both stability constants have been measured.[32,33] The calculated order of stability of complex formation with amino acids for both Cu^{2+} and Ni^{2+} depends on whether optimized or crystal structure geometries are used. Optimized geometries for β-alanine and Gaba complexes (Figures 4 and 5) indicate the presence of strong intramolecular interaction between an axially coordinated H_2O molecule and the free carbonyl oxygen of the amino acid, which enhances, their stability relative to α-amino acid complexes in which such interactions do not occur. This source of enhanced stability in favor of Gaba and β-alanine, however, would not be present in bulk water or in crystals where solvent or intermolecular interactions dominate.

Thus stabilities calculated from crystal structure rather than optimized geometries should be more relevant to observed solution behavior. These calculated values are found to be in qualitative agreement with observed stability constants for α-Ala > β-Ala and with the similar values of K_{I} and K_{II} reported for α-amino acids in solution. However, for Gaba complexes, for which there is no crystal structure, the com-

---

(32) Martell, A. E.; Smith, R. M. "Critical Stability Constants"; Plenum Press: New York, 1974; Vol. 1.

(33) Perrin, D. D. "Stability Constants of Metal Ion Complexes", Part B, IUPAC Chemical Data Series No. 22; Pergamon Press: New York, 1979.

Table VI. Mulliken Orbital Populations of the Metal (M) Orbitals in the 1:2 Metal–Amino Acid Complexes

	4s	$4p_x$	$4p_y$	$4p_z$	$3d_{z^2}$	$3d_{x^2-y^2}$	$3d_{xy}$	$3d_{xz}$	$3d_{yz}$
				M = Cu					
M-α-Ala[a]	0.2975	0.1243	0.2254	0.1746	1.9269	1.5095	1.9984	1.9990	1.9997
M-Sar[a]	0.2716	0.0816	0.2285	0.1575	1.9269	1.5172	1.9994	1.9991	1.9997
M-Aba[a]	0.3046	0.1252	0.2287	0.1703	1.9286	1.5125	1.9994	1.9992	1.9999
M-Aaib[a]	0.2976	0.1235	0.2343	0.1650	1.9125	1.5562	1.9937	1.9992	1.9998
M-Val[a]	0.3020	0.1297	0.2287	0.1747	1.9282	1.5025	1.9995	1.9990	1.9997
M-β-Ala[a]	0.2975	0.1232	0.2370	0.1569	1.9449	1.5379	1.9754	1.9984	1.9774
M-Gaba[a]	0.2890	0.1287	0.1865	0.1881	1.8513	1.5494	1.9988	1.9991	1.9996
				M = Ni					
M-α-Ala[a]	0.2877	0.1333	0.2189	0.1724	1.1098	1.2320	1.9987	1.9986	1.9994
M-Sar[a]	0.2681	0.1000	0.2171	0.1635	1.1113	1.2346	1.9975	1.9989	1.9994
M-Aba[a]	0.2878	0.1361	0.2178	0.1737	1.1089	1.2337	1.9974	1.9985	1.9994
M-Aaib[a]	0.2932	0.1309	0.2214	0.1683	1.1106	1.2350	1.9989	1.9986	1.9996
M-Val[a]	0.2870	0.1352	0.2177	0.1727	1.1088	1.2342	1.9976	1.9985	1.9994
M-β-Ala[a]	0.2501	0.1410	0.1876	0.1149	1.1209	1.2258	1.9943	1.9985	1.9951
M-Gaba[a]	0.2806	0.1212	0.2061	0.1722	1.1344	1.1896	1.9989	1.9985	1.9994

[a] The abbreviations for amino acids are the same as in Table I.

Table VII. Spin Densities in Metal (M)–Amino Acid Complexes

	1:1 complexes			1:2 complexes			
	d_{z^2}[a]	$d_{x^2-y^2}$[a]	O p_y[b]	d_{z^2}[a]	$d_{x^2-y^2}$[a]	O p_y[b]	O p_y[b]
			M = Cu				
$M(H_2O)_6{}^{2+}$		0.709					
M-α-Ala[c]		0.214	0.546		0.486	0.167	0.166
M-Sar[c]		0.207	0.540		0.478	0.168	0.168
M-Aba[c]		0.225	0.533		0.483	0.168	0.167
M-Aaib[c]		0.175	0.624		0.440	0.181	0.180
M-Val[c]		0.228	0.530		0.492	0.164	0.163
M-β-Ala[c]		0.209	0.411		0.457	0.127	0.127
M-Gaba[c]		0.441	0.250		0.463	0.147	0.147
			M = Ni				
$M(H_2O)_6{}^{2+}$	0.795	0.796					
M-α-Ala[c]	0.796	0.722	0.135	0.879	0.756	0.085	0.085
M-Sar[c]	0.814	0.733	0.133	0.878	0.753	0.084	0.084
M-Aba[c]	0.802	0.723	0.134	0.880	0.754	0.083	0.083
M-Aaib[c]	0.864	0.721	0.150	0.878	0.752	0.086	0.086
M-Val[c]	0.795	0.715	0.132	0.880	0.754	0.083	0.083
M-β-Ala[c]	0.804	0.805	0.059	0.870	0.766	0.079	0.079
M-Gaba[c]	0.815	0.818	0.068	0.856	0.798	0.057	0.074

[a] Metal d orbitals. [b] p_y orbital of the amino acid oxygen chelated to the metal. [c] The abbreviations for amino acids are the same as in Table I.

posite geometries used already contain these favorable intramolecular interactions, resulting in an overestimation of their relative stability.

While the calculated internal energy results are qualitatively consistent with the measured equilibrium constants in solution, the uncertainties in our method, the exponential dependence of equilibrium constants on free energy of reaction, and the neglect of entropy changes, which appear to be less favorable for longer chain amino acids, do not allow a quantitative prediction of the order of stability of complex formation in solution, particularly among different classes of amino acids.

One of the significant implications of our results is that, whether or not optimized geometries are used, the process of complex formation does not lead to the selection of biological subset from dilute solutions into the interlamellar region of homoionic clays. Results from crystal or composite geometries indicate that α-Ala forms the most stable 1:1 complex with Cu^{2+} and Ni^{2+} but that the complexes formed by valine are among the least stable. Using optimized geometries, we find that Aaib with two CH_3 groups on the α-carbon forms the most stable complex with the most planar five-membered chelate ring.

As noted earlier, the difference between the thermodynamics of complex formation in the interlamellar spacing of the clay and in the solution, within the limits of our treatment, is of the energy required to release a proton from the zwitterionic form of the amino acid to form an anion. However, this is not a constant energy, as is clear from Tables I and II; therefore, the use of solution stability constants to predict the specificities in clays could be misleading. The relative stability results obtained here by using eq 1, while not including explicit electronic effects of the clay in complex formation, more nearly correspond to the expected amino acid adsorption selectivity in clay if transition-metal complex formation is the determining process in such selectivity.

Another prediction from our results is that, if such complex formation is the major factor is governing amino acid adsorption, then only 1:1 complexes will be formed by α- and β-amino acids with the hexahydrated Cu^{2+} and Ni^{2+} cations in the interlamellar regions. Energies of reactions for 1:1 complexes of α- and β-amino acids are more exothermic than those for 1:2 complexes (Table I).

Moreover, only 1:1 α-amino acid complexes can be accomodated within the steric constraints of the clay (Figure 7). As discussed below, ESR measurements of Cu^{2+}–amino acid complexes in clays would help verify this prediction.

Other steric constraints also suggest that, despite favorable energetics, neither 1:1 nor 1:2 cation complexes with Gaba would form in the interlamellar region of homoionic clay. As shown in Figure 9, when the seven-membered-ring chelate formed by Gaba with Ni^{2+} or Cu^{2+} is placed in the interlamellar region of the clay, there is a close contact (1.9 Å) between the free carbonyl oxygen and two silicate oxygen atoms of the clay, which is smaller than the van der Waals radii of two oxygen atoms (~3 Å).

In addition to the energetics of complex formation by hydrated Cu^{2+} and Ni^{2+} cations, the nature of the electronic structure and spin distributions in the complexes formed by these two transition metals has been characterized.

As seen in Table III, there is considerable electron transfer to the metals even in their hexahydrated complexes, and the metal cation, with a 2+ formal charge, acquires about 1.1 e from the six water molecules. This charge transfer is accompanied by a polarization of the H_2O molecules, making the hydrogen atoms the ultimate electron donors. Replacement of two H_2O molecules by one amino acid anion, to form 1:1 complexes, enhances the total charge transfer both to Ni ($\simeq$1.2 e) and to Cu ($\simeq$1.4 e). The charge donation per water molecule from the four remaining H_2O molecules is reduced from 0.18 to $\simeq$0.10–0.14 e, while the anionic amino acid donates its full negative charge to Cu^{2+} but only $\simeq$0.6 e to Ni^{2+}. This difference in charge transfer to the two metals comes mainly from the difference in extent of electron transfer from the chelating carbonyl oxygen. The net charge on this oxygen of ~0.65– in the free amino acid anion is reduced to ~0.53– in Ni^{2+} and to ~0.36– in the Cu^{2+} complex. Charge transfer from the amino acid to the cation is accompanied by a large polarization of the amino acids, making the H atoms rather than the O and N ligand atoms the principal net electron donors. The calculated bond-overlap density, which is a measure of bond strength, indicates a weakening of the metal–water bond upon metal ion chelation with an amino acid. In Cu^{2+} and Ni^{2+} 1:1 complexes, the metal–nitrogen bond-overlap density is about the same, but the Cu–O bond overlap density is less than that for the Ni–O bond, indicating a more ionic bond for Cu–O, consistent with the larger amount of charge transfer from O to Cu^{2+} than to Ni^{2+}.

Surprisingly, in the 1:2 complexes (Table IV), there is no significant net increase in charge transfer to the metal ions compared to the case of the 1:1 complexes (Table III). In fact, while Ni retains about the same (+) charge in its 1:1 and 1:2 complexes, net charge transfer to the Cu is calculated to *decrease* in the 1:2 complex; and each amino acid in the 1:2 complex retains about half its negative charge.

In addition to differences in extent of charge transfer, the calculated electronic structure and spin distribution are qualitatively different in 1:1 and 1:2 complexes. As seen in Table V, the configuration of Cu^{2+} in its 1:1 complexes can be best described as d^{10}; i.e., electrons are donated from the ligand to Cu into a $d_{x^2-y^2}$ orbital as well as into vacant 4s and 4p orbitals. However, this situation is quite different in the 1:2 complexes. As shown in Table VI, the Cu configuration is best described as "d^9" with less electrons in the $d_{x^2-y^2}$ orbital. There is a back-donation of charge from this orbital to the two p orbitals of the chelating amino acid oxygen atoms. This back-donation results in slightly less charge transfer to the Cu and larger Cu–O (amino acid) bond-overlap density in 1:2 complexes (Table IV) compared to that in 1:1 complexes (Table III).

There is no such qualitative difference in the 1:1 and 1:2 Ni^{2+} complexes. On the assumption of a triplet ground state, Ni has an $\sim d^8(d_{z^2})^1(d_{x^2-y^2})^1(d_{xy})^2(d_{xz})^2(d_{yz})^2$ configuration in both types of complexes with charge transfer mainly to the 4s and 4p orbitals.

The electron distributions given in Tables III and V are mirrored in the spin distributions given in Table VII. As shown in this table, the Cu^{2+} ion in its hexahydrated complexes is predicted to have considerable spin density (71%) consistent with the observation of a typical anisotropic copper ESR spectrum.

In all of the Cu 1:1 complexes with amino acids, however, most of the spin density is calculated to shift to the oxygen ligand of the amino acid, leaving 17–23% electron density in the Cu^{2+}. In the 1:2 complexes more spin density is retained on the Cu^{2+} (~48%). Thus if, as predicted, Cu^{2+} forms 1:1 complexes in homoionic clays, an isotropic ESR signal with $g \sim 2$ typical of a free radical (O·) should be observed; but if it forms 1:2 complexes, a typical anisotropic Cu signal shold also be seen.

There is some evidence for such a change in Cu^{2+} hydrated spectra upon complex formation with benzene in homoionic clays. The intial ESR spectrum observed corresponds to a typical Cu^{2+} signal, i.e., $g_{\parallel} = 2.34$ and $g_{\perp} = 2.08$, while a subsequent one corresponds to a free radical signal, i.e., $g = 2.003$.[34,35] Similar ESR experiments for amino acid complexes with Cu^{2+} in homoionic clays could serve as a probe of the stoichiometry and help verify the prediction that only 1:1 complexes would be formed and that in these complexes Cu is in a "d^{10}" configuration with the main unpaired spin density on the oxygen ligand.

Conclusion

In this study, the binding of Gaba, β-alanine, and five α-amino acids, alanine and valine (biological subset) and sarcosine, Aba, and Aaib (nonbiological subset), in their zwitterionic and anionic forms, to hydrated Cu^{2+} and Ni^{2+} has been characterized by using semiempirical molecular orbital methods. The results for complex formation with the anionic amino acids predict stable 1:1 and 1:2 complexes. Cu^{2+} complexes are found to be energetically favored over those of Ni^{2+}, and an order of stability is predicted for α- and β-amino acids, which is in qualitative agreement with observed solution behavior.

Stable 1:1 complexes were also formed with the zwitterionic form of the amino acids, a process assumed to occur in the interlamellar region of the homoionic clays. However, from both steric and energy considerations, 1:2 complexes are predicted not to form in the clay. The calculated electronic structure and spin distribution of metal ion–amino acid complexes suggests that ESR techniques can be used to verify the predicted 1:1 stoichiometry of the complexes formed in clays.

Steric constraints do not appear to allow Gaba to bind as either a 1:1 or a 1:2 chelated complex in the interlamellar region of homionic clays.

Neither Cu^{2+} nor Ni^{2+} was found to preferentially select the biological subset of amino acids, α-Ala and valine, for complex formation.

Acknowledgment. The authors are grateful to Gail Hashimoto for her help in preparing the computer graphics generated complexes and clay surfaces. Financial support for this work by NASA-Ames Consortium Agreement No. NCC2-96 is gratefully acknowledged.

Registry No. Cu, 7440-50-8; Ni, 7440-02-0; α-Ala, 56-41-7; Val, 72-18-4; Sar, 107-97-1; Aba, 80-60-4; Aaib, 62-57-7; β-Ala, 107-95-9; Gaba, 56-12-2.

---

(34) Mortland, M. M.; Pinnavaia, T. J. *Nature (London), Phys. Sci.* **1971**, *299*, 75–72.

(35) Mortland, M. M; Halloran, J. T. *Soil Sci. Soc. Am. J.* **1976**, *40*, 367–370.